

Dartmouth College Dartmouth Digital Commons

Dartmouth Faculty Open Access Articles

Open Dartmouth: Faculty Open Access

6-23-2015

Resonance of relativistic electrons with electromagnetic ion cyclotron waves

Richard Denton
Dartmouth College

K. Jordanova
Los Alamos National Laboratory

J. Bortnik
University of California, Los Angeles

Follow this and additional works at: <http://digitalcommons.dartmouth.edu/facoa>

 Part of the [Geophysics and Seismology Commons](#)

Recommended Citation

Denton, Richard; Jordanova, K.; and Bortnik, J., "Resonance of relativistic electrons with electromagnetic ion cyclotron waves" (2015). *Dartmouth Faculty Open Access Articles*. 53.
<http://digitalcommons.dartmouth.edu/facoa/53>

This Article is brought to you for free and open access by the Open Dartmouth: Faculty Open Access at Dartmouth Digital Commons. It has been accepted for inclusion in Dartmouth Faculty Open Access Articles by an authorized administrator of Dartmouth Digital Commons. For more information, please contact dartmouthdigitalcommons@groups.dartmouth.edu.

1 Resonance of relativistic electrons with
2 electromagnetic ion cyclotron waves

R. E. Denton¹, V. K. Jordanova², J. Bortnik³

J. Bortnik, Mathematical Sciences Building, Rm 7115, UCLA, Los Angeles, CA, 90095-1565, USA. (jbortnik@gmail.com)

R. E. Denton, 32 Oak Tree Dr., New Smyrna Beach, FL 32169, USA. (richard.e.denton@dartmouth.edu)

V. K. Jordanova, Los Alamos National Lab, MS D466, Los Alamos, NM 87545-0000, USA. (vania@lanl.gov)

¹Department of Physics and Astronomy,
Dartmouth College, Hanover, New
Hampshire, USA

²Los Alamos National Lab, Los Alamos,
New Mexico, USA

³Department of Atmospheric and Oceanic
Sciences, University of California Los
Angeles, Los Angeles, CA, USA

3 Relativistic electrons have been thought to more easily resonate with elec-
4 tromagnetic ion cyclotron (EMIC) waves if the total density is large. We show
5 that, for a particular EMIC mode, this dependence is weak due to the de-
6 pendence of the wave frequency and wave vector on the density. A signifi-
7 cant increase in relativistic electron minimum resonant energy might occur
8 for the H band EMIC mode only for small density, but no changes in param-
9 eters significantly decrease the minimum resonant energy from a nominal value.
10 The minimum resonant energy depends most strongly on the thermal veloc-
11 ity associated with the field line motion of the hot ring current protons that
12 drive the instability. High density due to a plasmasphere or plasmaspheric
13 plume could possibly lead to lower minimum resonance energy by causing
14 the He band EMIC mode to be dominant. We demonstrate these points us-
15 ing parameters from a ring current simulation.

1. Introduction

16 Relativistic electrons are commonly thought to strongly interact with magnetospheric
 17 waves when they are in resonance [*Kennel and Petschek, 1966; Shprits et al., 2008; Albert*
 18 *and Bortnik, 2009*]. The resonance condition is

$$19 \quad \omega - k_{\parallel} v_{\parallel} = -n \frac{\Omega_{ce}}{\gamma}, \quad (1)$$

20 where ω is the wave frequency; k_{\parallel} is the component of the wave vector parallel to the
 21 background magnetic field; v_{\parallel} is the parallel component of the relativistic electron velocity
 22 v ; n is the order of the resonance; $\Omega_{ce} = eB/m_e$ is the nonrelativistic electron cyclotron
 23 frequency, where e is the absolute value of the electron charge, B is the background
 24 magnetic field, and m_e is the electron rest mass; and $\gamma = 1/\sqrt{1 - (v/c)^2}$ is the relativistic
 25 factor for the electron.

26 Here we want to consider resonance with electromagnetic ion cyclotron (EMIC) waves
 27 [*Cornwall, 1965; Kennel and Petschek, 1966; Anderson et al., 1996; Meredith et al., 2003;*
 28 *Denton et al., 2014; Li et al., 2014*]. We want to find the lowest energy relativistic electron
 29 that can resonate with the waves. EMIC waves are predominantly transverse, but as the
 30 waves propagate away from the magnetic equator, they can become oblique and develop
 31 a nonzero parallel electric field. In that case the so called Landau resonance with $n = 0$
 32 might occur, but that interaction would be with low energy electrons with parallel velocity
 33 comparable to the Alfvén speed. The lowest energy interaction with relativistic electrons
 34 would occur for $n = 1$; for $n = 1$, v_{\parallel} has the same sign as k_{\parallel} in (1), indicating that the
 35 resonant electrons move in the same direction as the wave. Henceforth, we will consider
 36 only this $n = 1$ resonance.

EMIC waves have real frequency below the proton gyrofrequency. Thus, unless γ in (1) is extremely large, ω in (1) will be utterly negligible compared to Ω_{ce}/γ . This means that the relativistic electrons are moving so fast that on the time scale of their motion through the waves, the EMIC waves are essentially static.

The lowest energy particle satisfying (1) would be moving parallel to the background magnetic field \mathbf{B} , so that $v_{\parallel} = v = c\sqrt{1 - 1/\gamma^2}$. Then, dropping the ω term in (1), the minimum energy particle having $\gamma = \gamma_{\min}$ would have

$$\bar{p}_{\min} \equiv \gamma_{\min} \frac{v_{\min}}{c} = \gamma_{\min} \sqrt{1 - \frac{1}{\gamma_{\min}^2}} = \frac{\Omega_{ce}}{ck_{\parallel}}. \quad (2)$$

The quantity \bar{p}_{\min} is the minimum relativistic momentum of the electron p_{\min} normalized to $m_e c$; $\bar{p}_{\min} \approx \gamma_{\min}$ for large γ_{\min} , but $\bar{p}_{\min} \approx v/c$ as γ_{\min} approaches unity. The value of \bar{p}_{\min} monotonically increases with respect to the total energy of the electron, $\gamma_{\min} m_e c^2$, and therefore also monotonically increases with respect to the kinetic energy of the electron $E_{K,\min} = (\gamma_{\min} - 1)m_e c^2$. So the larger the value of k_{\parallel} (shorter wavelength), the smaller the value of \bar{p}_{\min} corresponding to smaller $E_{K,\min}$. Given \bar{p}_{\min} , $\gamma_{\min} = \sqrt{1 + \bar{p}_{\min}^2}$, and therefore

$$E_{K,\min} = \left(\sqrt{1 + \bar{p}_{\min}^2} - 1 \right) m_e c^2 \quad (3)$$

[see also *Silin et al.*, 2011].

For a multi-species plasma with singly charged ions of species s , the dispersion relation for electromagnetic ion cyclotron waves is [*Swanson*, 2003; *Denton et al.*, 2014]

$$\bar{k}_{\parallel}^2 = \bar{\omega} \left(\sum_s \frac{\eta_s}{1 - \bar{m}_s \bar{\omega}} - 1 \right). \quad (4)$$

57 Here the overbars indicate normalized quantities, where we have normalized distances to
 58 c/ω_{pp} and inverse time to Ω_{cp} ; the proton plasma frequency is $\omega_{\text{pp}} \equiv \sqrt{n_e e^2 / m_p \epsilon_0}$; the
 59 proton cyclotron frequency is $\Omega_{\text{cp}} \equiv eB/m_p$; n_e is the electron density; m_p is the proton
 60 mass; ϵ_0 is the vacuum permittivity; the ion species concentration $\eta_s \equiv n_s/n_e$; and the
 61 normalized ion mass $\bar{m}_s \equiv m_s/m_p$. Using the normalized $\bar{k}_{\parallel} \equiv k_{\parallel} c/\omega_{\text{pp}}$, (2) can be written
 62 as

$$63 \quad \bar{p}_{\text{min}} = \frac{\Omega_{\text{ce}}}{\omega_{\text{pp}}} \frac{1}{\bar{k}_{\parallel}} = \sqrt{\frac{m_p}{m_e}} \frac{\Omega_{\text{ce}}}{\omega_{\text{pe}}} \frac{1}{\bar{k}_{\parallel}}, \quad (5)$$

64 where $\omega_{\text{pe}} \equiv \sqrt{n_e e^2 / m_e \epsilon_0}$ is the electron plasma frequency.

65 If one assumes that the EMIC waves have a certain normalized frequency, $\bar{\omega} \equiv \omega/\Omega_{\text{cp}}$,
 66 independent of the value of $\omega_{\text{pp}} \propto \sqrt{n_e}$, then (4) shows that \bar{k}_{\parallel} will also not depend on
 67 ω_{pp} . Then (5) shows that \bar{p}_{min} will be proportional to $n_e^{-1/2}$. This indicates that larger
 68 total density will allow lower energy electrons to resonate with the EMIC waves, and this
 69 is one reason that the outer plasmasphere and plasmaspheric plume are considered to be
 70 good locations for interaction between EMIC waves and relativistic electrons.

71 But recently, *Denton et al.* [2014] showed that $\bar{\omega}$ decreases with respect to n_e in a way
 72 that can be described by a simple formula (their equation (6) and our equation (8) derived
 73 in section 2). If $\bar{\omega}$ decreases with respect to n_e , (4) shows that \bar{k}_{\parallel} also generally decreases
 74 with respect to n_e (except very near resonances [*Denton et al.*, 2014]). The \bar{k}_{\parallel} dependence,
 75 decreasing with respect to n_e , will thus tend to counteract the ω_{pe} dependence, increasing
 76 with respect to n_e , in (5).

77 In this paper, we will examine the dependence of \bar{p}_{min} on n_e as well as on the ion species
 78 concentrations η_s , in order to better understand the conditions under which relativistic

79 electrons most easily resonate with EMIC waves. We find that for a particular EMIC wave
 80 mode, \bar{p}_{\min} depends most strongly on the hot ring current thermal velocity associated
 81 with parallel motion, $v_{\text{th}\parallel\text{h}}$ (defined below). In section 2 we will show our results, and in
 82 section 3, we will discuss and summarize these results.

2. Dependence of \bar{p}_{\min} on density and ion composition

83 *Denton et al.* [2014] assumed that EMIC waves are driven by a bi-Maxwellian dis-
 84 tribution of hot ring current protons such that the wave is in Doppler resonance with
 85 Ω_{cp} for the hot protons with a parallel velocity equal to their parallel thermal speed,
 86 $v_{\text{th}\parallel\text{h}} \equiv \sqrt{2k_B T_{\parallel\text{h}}/m_p}$, moving in the direction opposite to that of the wave (k_{\parallel} and v_{\parallel} in
 87 (1) have opposite sign), so that

$$88 \quad \omega + k_{\parallel} v_{\text{th}\parallel\text{h}} = \Omega_{\text{cp}}. \quad (6)$$

89 Here k_B is the Boltzmann constant, and $T_{\parallel\text{h}}$ is the hot proton temperature associated
 90 with motion along the magnetic field. Equation (6) can be written as

$$91 \quad \bar{k}_{\parallel} \sqrt{\beta_{\parallel\text{h,e}}} = 1 - \bar{\omega}, \quad (7)$$

92 where $\beta_{\parallel\text{h,e}} \equiv n_e k_B T_{\parallel\text{h}} / (B^2 / (2\mu_0))$ is the hybrid plasma beta calculated using the parallel
 93 temperature of the hot protons with the total electron density n_e ; it could also be written
 94 as $\beta_{\parallel\text{h}} n_e / n_h$, where $\beta_{\parallel\text{h}}$ is the plasma beta of the hot ring current protons defined using
 95 the parallel temperature.

96 Combining (7) with (4), Denton et al. found

$$97 \quad \frac{\bar{\omega}}{(1 - \bar{\omega})^2} \left(\sum_s \frac{\eta_s}{1 - \bar{m}_s \bar{\omega}} - 1 \right) = \frac{1}{\beta_{\parallel\text{h,e}}}, \quad (8)$$

98 and they showed that this equation well predicted the most unstable frequencies of EMIC
 99 waves using plasma parameters from a ring current simulation of an event during which
 100 EMIC waves were observed. For detailed information about this simulation, see the
 101 description of *Denton et al.* [2014]; for our purposes here, the parameters shown in Figure 1
 102 for Denton et al.'s "constant cold composition" simulation will be sufficient for a sample
 103 case. For an H+/He+/O+ plasma, EMIC waves occur in three bands, the H band, the He
 104 band, and the O band, where the frequency of the band approaches the gyrofrequency of
 105 the named ion species (for a cold plasma) for large k_{\parallel} . Figure 1d shows $\bar{\omega} \equiv \omega/\Omega_{cp}$ for the
 106 H and He band EMIC modes (from Figure 10a of *Denton et al.* [2014]). The solid curves
 107 in Figure 1d show the prediction of the simple model in (8), while the asterisks were found
 108 from kinetic theory, and the "o" symbols were found from a hybrid code simulation. The
 109 rough agreement of these different symbols validates the assumption of (6).

110 We can rearrange (5) to get

$$111 \quad \bar{p}_{\min} = \left(\frac{m_p}{m_e} \frac{v_{th\parallel h}}{c} \right) \left(\frac{1}{\bar{k}_{\parallel} \sqrt{\beta_{\parallel h,e}}} \right) \quad (9)$$

$$112 \quad = \left(\frac{m_p}{m_e} \frac{v_{th\parallel h}}{c} \right) \left(\frac{1}{1 - \bar{\omega}} \right), \quad (10)$$

113 where we used (7) to find (10). In (9) or (10), the terms in the left parentheses depend
 114 only on $v_{th\parallel h}$, or equivalently, on $T_{\parallel h}$. Only the terms in the second parentheses depend
 115 on n_e . Also, $\beta_{\parallel h,e} \propto n_e$. Therefore, we can see the dependence of \bar{p}_{\min} on n_e by plotting
 116 $\left(\bar{k}_{\parallel} \sqrt{\beta_{\parallel h,e}} \right)^{-1}$, or equivalently, $(1 - \bar{\omega})^{-1}$, versus $\beta_{\parallel h,e}$. We will discuss the dependence on
 117 $v_{th\parallel h}$ in section 3.

118 The dependence of \bar{p}_{\min} on $\bar{\omega}$ in (10) is the opposite of many people's expectation.
 119 Larger $\bar{\omega}$ leads to larger \bar{p}_{\min} . We emphasize that if $\bar{\omega}$ could be varied independently of

120 the plasma parameters, then larger $\bar{\omega}$ would correspond to larger \bar{k}_{\parallel} (from equation (4)).
 121 But we are assuming that the ring current protons must be in resonance with the wave.
 122 Then (6) shows that higher frequency corresponds to smaller wave number, given that
 123 $v_{\text{th}\parallel\text{h}}$ is held constant.

124 The term $(\bar{k}_{\parallel}\sqrt{\beta_{\parallel\text{h,e}}})^{-1} = (1 - \bar{\omega})^{-1}$ can only be large if $\bar{\omega}$ approaches unity. This
 125 means that the only mode for which $(\bar{k}_{\parallel}\sqrt{\beta_{\parallel\text{h,e}}})^{-1}$ could possibly deviate greatly from
 126 unity is the H band EMIC mode. Note that for the He band EMIC mode, the variation
 127 of $(1 - \bar{\omega})^{-1}$ could only range between 16/15 for $\bar{\omega} = 1/16$ (He band cutoff frequency at
 128 the O+ gyrofrequency) to 4/3 for $\bar{\omega} = 1/4$ at the He+ gyrofrequency resonance, a total
 129 range of a factor of 1.25.

130 We now choose these nominal parameters, $\beta_{\parallel\text{h,e}} = 10$, $\eta_{\text{He}+} = 0.1$, and $\eta_{\text{O}+} = 0.01$ for
 131 an H+/He+/O+ plasma. Keeping one or two of these parameters constant and varying
 132 the other parameters, we will examine the resulting variation in \bar{p}_{min} . In each case,
 133 $\eta_{\text{H}+} = 1 - \eta_{\text{He}+} - \eta_{\text{O}+}$; $\bar{\omega}$ is found from (8) using a numerical root solver; and \bar{k}_{\parallel} is found
 134 from (4).

2.1. Density dependence

135 Keeping $\eta_{\text{He}+} = 0.1$ and $\eta_{\text{O}+} = 0.01$, we plot $\bar{\omega}$, \bar{k}_{\parallel} , and $(1 - \bar{\omega})^{-1} = (\bar{k}_{\parallel}\sqrt{\beta_{\parallel\text{h,e}}})^{-1}$ versus
 136 $\beta_{\parallel\text{h,e}}$ in Figure 2 for the H band EMIC mode (black solid curve), the He band EMIC mode
 137 (blue curve), and the O band EMIC mode (red curve). Note that the cutoff frequencies
 138 occur at the right side of the plot, where \bar{k}_{\parallel} is small, and the resonance frequencies are
 139 approached at the left side of the plot.

140 As noted previously, $\bar{\omega}$ decreases with respect to $\beta_{\parallel h,e} \propto n_e$ for each mode (Figure 2a).
 141 Consequently, \bar{k}_{\parallel} decreases with respect to $\beta_{\parallel h,e}$ for each mode (Figure 2b). The value of
 142 \bar{k}_{\parallel} is nearly proportional to $\beta_{\parallel h,e}^{-0.5}$ (slope of diagonal dotted black line in Figure 2b). As
 143 suggested by (7), large departures from this relationship only occur where $\bar{\omega}$ approaches
 144 unity.

145 Therefore, as noted above, the largest variation in $(1 - \bar{\omega})^{-1} = (\bar{k}_{\parallel} \sqrt{\beta_{\parallel h,e}})^{-1}$ is for the
 146 H band EMIC mode (black solid curve in Figure 2c), and particularly for $\beta_{\parallel h,e} < 1$. In
 147 that case, low values of $\beta_{\parallel h,e}$ lead to large values of \bar{p}_{\min} , indicating that it is more difficult
 148 for low energy relativistic electrons to resonate with the waves. But the EMIC mode may
 149 not be unstable for such small values of $\beta_{\parallel h,e}$ [Blum *et al.*, 2009].

150 Note also that $(1 - \bar{\omega})^{-1}$ is lower for He band EMIC than for H band EMIC, indicating
 151 that it is easier for low energy relativistic electrons to resonate with the He band waves.
 152 This is because, given the same value of $v_{\text{th}\parallel h}$, a larger value of k_{\parallel} is required to Doppler
 153 shift the wave frequency up to Ω_{cp} from the lower frequency (equation (6)). (It would
 154 be even easier for low energy relativistic electrons to resonate with O band waves, but O
 155 band waves are not as common as waves in the H and He bands.)

2.2. Composition dependence

156 Figure 3 shows the same quantities that were plotted in Figure 2, but plotted versus
 157 η_{He^+} holding $\eta_{\text{O}^+} = 0.01$ constant in column a, and versus η_{O^+} holding $\eta_{\text{He}^+} = 0.1$ constant
 158 in column b. In both cases, $\beta_{\parallel h,e} = 10$ is constant. With $\beta_{\parallel h,e}$ constant, (9) shows that
 159 the concentration of ions species η_s affects the value of \bar{p}_{\min} through the term $(1 - \bar{\omega})^{-1}$.

160 The presence of heavy ions (heavier than the species name for the EMIC wave band)
 161 leads to an increase in $\bar{\omega}$ [Denton *et al.*, 2014]. From Figure 3Ca and Cb, we see that
 162 $(1 - \bar{\omega})^{-1}$ is close to unity except for the H band EMIC mode at large values of heavy
 163 ion concentration. In that case, large concentration of He+ or O+ leads to large values
 164 of \bar{p}_{\min} , indicating that it is more difficult for low energy relativistic electrons to resonate
 165 with the waves.

3. Discussion

166 We have shown that the minimum resonant energy, characterized by $\bar{p}_{\min} \equiv$
 167 $\gamma_{\min} \sqrt{1 - \frac{1}{\gamma_{\min}^2}} \propto (\bar{k}_{\parallel} \sqrt{\beta_{\parallel h,e}})^{-1} = (1 - \bar{\omega})^{-1}$ (equations (2), (9), and (10)), is only weakly
 168 dependent on $\beta_{\parallel h,e} \propto n_e$ (Figure 2) and the heavy ion concentrations $\eta_{\text{He}+}$ (Figure 3Ca)
 169 and $\eta_{\text{O}+}$ (Figure 3Cb) for a particular wave mode. The only significant dependence on
 170 these quantities is for the H band EMIC mode. For that mode, the strongest dependence
 171 on $\beta_{\parallel h,e}$ is for very low values, but at very low values of $\beta_{\parallel h,e}$, EMIC waves may not be
 172 unstable [Blum *et al.*, 2009]. The heavy ions only have a significant effect at large $\eta_{\text{He}+}$ or
 173 $\eta_{\text{O}+}$. For $\sqrt{\beta_{\parallel h,e}}$ or η_s , strong dependence only occurs as $\bar{\omega}$ approaches unity. But in order
 174 for EMIC waves to grow with large $\bar{\omega}$, the temperature anisotropy of the hot ring current
 175 protons, $A_h \equiv T_{\perp h}/T_{\parallel h} - 1$, must be large. From Equation 2.23 of Kennel and Petschek
 176 [1966], $A_h \geq \bar{\omega}/(1 - \bar{\omega})$. So, for instance, $\bar{\omega} = 0.8$ would require $A_h = 4$ or $T_{\perp h}/T_{\parallel h} = 5$,
 177 which is rare.

178 Large $\bar{\omega}$ leads to large \bar{p}_{\min} making resonance with relativistic electrons more difficult.
 179 Variations in $\beta_{\parallel h,e}$, $\eta_{\text{He}+}$, and $\eta_{\text{O}+}$ do not cause large decreases in $(\bar{k}_{\parallel} \sqrt{\beta_{\parallel h,e}})^{-1} = (1 - \bar{\omega})^{-1}$.
 180 The maximum value of $\bar{k}_{\parallel} \sqrt{\beta_{\parallel h,e}}$ occurs with the lowest possible value of $\bar{\omega}$, meaning that

181 the Doppler term must shift the wave frequency up by the maximum amount (equation
 182 (6)). But the value of $\bar{\omega}$ will be at least zero, leading to $(1 - \bar{\omega})^{-1} = 1$. For the He
 183 band EMIC mode, often thought to be most important for relativistic electron pitch
 184 angle scattering, $(1 - \bar{\omega})^{-1}$ is always close to unity since $\bar{\omega}$ varies only between $1/16$ (O+
 185 gyrofrequency) and $1/4$ (He+ gyrofrequency).

186 Based on these facts, the largest dependence of \bar{p}_{\min} for a particular mode is not on
 187 $\beta_{\parallel h,e} \propto n_e$, $\eta_{\text{He}+}$, or $\eta_{\text{O}+}$, but on $v_{\text{th}\parallel h} \propto \sqrt{T_{\parallel h}}$ (equation (9) or (10)), since $\bar{p}_{\min} \propto$
 188 $v_{\text{th}\parallel h}$. That is, it is the parallel temperature of the hot ring current protons driving
 189 the EMIC waves that has the greatest impact on the minimum resonant energy. If low
 190 energy ring current protons drive the EMIC instability, it will be easier for low energy
 191 relativistic electrons to resonate with the waves. A rough approximation to (9), $\gamma =$
 192 $(m_p/m_e)(v_{\text{th}\parallel h}/c)$, follows directly from approximating the ion and electron resonance
 193 conditions as $k_{\parallel}v_{\text{th}\parallel h} = \Omega_{cp}$ and $k_{\parallel}c = \Omega_{ce}/\gamma$, respectively; that is, $\bar{\omega}$ in (10) is taken to
 194 be zero.

195 Now consider again the parameters from the ring current simulation described by *Denton*
 196 *et al.* [2014] and plotted in Figure 1. Figure 1e shows \bar{p}_{\min} for the H band mode (black
 197 curve) and He band mode (blue curve) calculated using (10) with the hot H+ parallel
 198 temperature $T_{\parallel h}$ from Figure 1a and the normalized wave frequency $\bar{\omega}$ in Figure 1d. The
 199 lowest value of \bar{p}_{\min} is for the He band EMIC mode, which is also the largest mode growing
 200 in the the hybrid code simulation [*Denton et al.*, 2014]. Note from the densities plotted
 201 in Figure 1b that the two gray vertical lines roughly delineate the plasmopause, with the
 202 plasmasphere to the left of the leftmost gray vertical line, and the plasmatrough to the

right of the rightmost gray vertical line. Despite the fact that the total density is much greater in the plasmasphere, \bar{p}_{\min} is smallest in the plasmatrrough (region to the right of the rightmost gray vertical line in Figure 1b). This is evidently because of the decrease in $T_{\parallel h}$ shown in Figure 1a.

Figure 1f shows the minimum resonant relativistic electron kinetic energy $E_{K,\min}$ calculated using \bar{p}_{\min} in (3) for the H band EMIC mode (black solid curve) and He band EMIC mode (blue solid curve). Again, the minimum resonant energy is lower for the He band mode and decreases at large L . To emphasize the functional dependence due to $T_{\parallel h}$ and $\bar{\omega}$, the dotted blue curve is plotted using variation in $T_{\parallel h}$, but holding $\bar{\omega}$ constant = 0.201, while the large dashed blue curve is plotted using variation in $\bar{\omega}$, but holding $T_{\parallel h}$ constant = 7.08 keV. While the $\bar{\omega}$ dependence does lead to a small decrease in $E_{K,\min}$ at low L (large dashed blue curve), the variation in $E_{K,\min}$ due to variation in $T_{\parallel h}$ is much larger (dotted blue curve).

Based on these results, if the plasmasphere or plasma plume is a preferred region for resonance of relativistic electrons with EMIC waves, as suggested by *Borovsky et al.* [2014], it's probably not because the cold density makes resonance easier, at least for a particular mode. As mentioned in the Introduction, if the normalized frequency of the waves, $\bar{\omega}$, were independent of n_e , then the minimum resonant energy would be significantly lower at high n_e . But *Denton et al.* [2014] showed that $\bar{\omega}$ decreases with respect to n_e ; and we have shown that this causes the minimum resonant energy to vary only very weakly with respect to n_e .

224 Values of $E_{K,\min}$ based on the finite temperature kinetic dispersion code Waves in Homo-
 225 geneous Anisotropic Multicomponent Plasmas (WHAMP) [Ronnmark, 1982] are shown
 226 in Figure 1f for the He mode at $L = 5.5$ and 6 (blue asterisks) and for the H mode at
 227 $L = 6.5$ (black asterisk) at the wave number for which the growth rate normalized to Ω_{cp} ,
 228 $\bar{\gamma}$, has its maximum value, $\bar{\gamma}_{\max}$. These results are generally in agreement with the simple
 229 model (solid curves in Figure 1f).

230 Two other recent papers have examined the relativistic electron resonance condition
 231 using kinetic theory [Silin *et al.*, 2011; Chen *et al.*, 2011]. Both of these claim that high
 232 density leads to a lower minimum resonant energy. Chen *et al.* evaluate the minimum
 233 resonant energy for all wave frequencies for which $\bar{\gamma}$ is greater than 0.01. The assumption
 234 is that a range of frequencies can be excited, and that the entire spectrum needs to
 235 be considered. While it's certainly true that the full spectrum of waves can resonate
 236 with relativistic electrons [Ukhorskiy *et al.*, 2010], it's not totally clear how to calculate
 237 the nonlinear spectrum of waves based on linear theory. At the least, this will depend
 238 sensitively on the initial noise level from which the waves grow.

239 Also, when parameters are varied independently, unrealistic combinations may result.
 240 For instance, the majority of cases described by Silin *et al.* [2011] have unrealistically
 241 high plasma beta. In their sweep of parameter space, Chen *et al.* [2011] do not mention
 242 the range of any parameter indicating instability [like that of Blum *et al.*, 2009], but
 243 given the range of parameter space explored, some of the cases considered may have been
 244 unrealistically unstable.

245 Larger growth rate leads to a greater range of frequencies that are unstable, and the
 246 higher frequencies, corresponding to larger wave number (not necessarily satisfying (6)),
 247 will have lower minimum resonant energy. *Chen et al.* [2011] find a correlation between
 248 increasing hot proton density n_h , hot proton temperature anisotropy, $A_h \equiv T_{\perp h}/T_{\parallel h} - 1$,
 249 and total density with lower minimum resonant energy. We find using WHAMP (not
 250 shown) that there is only a small change in $E_{K,\min}$ at $\bar{\gamma} = \bar{\gamma}_{\max}$ when the cold ion densities
 251 are increased, and that there is almost no change in $E_{K,\min}$ at $\bar{\gamma} = \bar{\gamma}_{\max}$ when n_h or A_h are
 252 increased. These results are consistent with the simple theory we have presented. But an
 253 increase in total density, n_h , or A_h , does lead to a more unstable plasma, yielding lower
 254 $E_{K,\min}$ within the range of unstable frequencies.

255 A more realistic way to vary the parameters might be to keep the instability condition
 256 [*Blum et al.*, 2009] roughly constant. The ring current parameters tend to be regulated
 257 close to a marginal stability condition [*Gary et al.*, 1994; *Denton et al.*, 1994; *Blum et al.*,
 258 2009]. For this reason, we have concentrated on the most unstable mode. We expect this
 259 mode to be the most intense, and hence to do the majority of the scattering [*Bortnik*
 260 *et al.*, 2010].

261 Relativistic electron precipitation events observed by balloons tend to be clustered
 262 around dusk local time. The relation $\bar{p}_{\min} \propto v_{th\parallel h}$ would suggest that low energy electrons
 263 might more easily resonate with EMIC waves at dawn or pre-dawn local time, where
 264 the ring current protons are typically of lower energy [*Anderson et al.*, 1996; *Lee and*
 265 *Angelopoulos*, 2014]. But there are other factors that come into play, such as higher con-

266 centration of O+ at dawn [*Denton et al.*, 2012; *Lee and Angelopoulos*, 2014] and better
267 conditions for growth of large amplitude waves at dusk [*Denton et al.*, 2014].

268 Theoretically, enhanced resonance of relativistic electrons with EMIC waves in the plas-
269 masphere or plume could result from larger growth of EMIC waves when the bulk density
270 is large [*Jordanova et al.*, 2008; *Denton et al.*, 2014]. There is some support for a cor-
271 relation between plasma density and EMIC waves, though the result is not unequivocal
272 [*Fraser et al.*, 2005; *Halford et al.*, 2015; *Usanova et al.*, 2013]. We are not aware of a study
273 showing that $T_{\parallel h}$ is normally lower in the plasmasphere or plume, and such a correlation
274 is not supported by the ring current simulation results plotted in Figure 1a, for which $T_{\parallel h}$
275 is greater in the plasmasphere.

276 High density at dusk is particularly conducive to producing He mode EMIC waves
277 [*Denton et al.*, 2014; *Lee and Angelopoulos*, 2014]. Figure 1f shows that $E_{K,\min}$ is lower
278 for He band EMIC than for H band EMIC. So if high density causes the He mode to be
279 dominant, that would lead to lower minimum resonance energies. In fact, the He band
280 EMIC mode is stable for the plasma parameters in Figure 1 outside the plasmopause at
281 $L = 6.5$. So considering the available wave modes, the minimum resonance energy is lower
282 at $L = 5.5$ than at $L = 6.5$ (comparing the blue asterisk at $L = 5.5$ in Figure 1f to the
283 black asterisk at $L = 6.5$).

284 It is also possible that non-resonant interactions could significantly affect the radiation
285 belt electrons. More work needs to be done to examine the pitch angle scattering of
286 relativistic electrons in realistic EMIC wave fields.

287 **Acknowledgments.** We thank Mary Hudson and Jay Albert for useful conversations.
288 Work at Dartmouth was supported by NASA grants NNX10AQ60G, NNX13AD65G, and
289 NNX08AM58G. Work at Los Alamos was conducted under the auspices of the U. S.
290 Department of Energy with partial support from NASA grant NNH13AW83I and NSF
291 grant IAA1203460. JB would like to acknowledge support from NSF/DOE basic plasma
292 physics grant DE-SC0010578. Numerical data shown in this paper are available from the
293 lead author upon request.

References

- 294 Albert, J. M., and J. Bortnik (2009), Nonlinear interaction of radiation belt electrons
295 with electromagnetic ion cyclotron waves, *Geophys. Res. Lett.*, p. L12110 (5 pp.), doi:
296 10.1029/2009gl038904.
- 297 Anderson, B. J., R. E. Denton, G. Ho, D. C. Hamilton, S. A. Fuselier, and R. J. Strangeway
298 (1996), Observational test of local proton cyclotron instability in the earth's magneto-
299 sphere, *J. Geophys. Res.*, 101(A10).
- 300 Blum, L. W., E. A. MacDonald, S. P. Gary, M. F. Thomsen, and H. E. Spence (2009),
301 Ion observations from geosynchronous orbit as a proxy for ion cyclotron wave growth
302 during storm times, *J. Geophys. Res.*, 114, doi:10.1029/2009ja014396.
- 303 Borovsky, J. E., R. H. W. Friedel, and M. H. Denton (2014), Statistically measuring the
304 amount of pitch angle scattering that energetic electrons undergo as they drift across
305 the plasmaspheric drainage plume at geosynchronous orbit, *J. Geophys. Res.*, 119(3),
306 1814–1826, doi:10.1002/2013ja019310.

- 307 Bortnik, J., R. M. Thorne, and N. Omidi (2010), Nonlinear evolution of EMIC waves in
308 a uniform magnetic field: 2. Test-particle scattering, *J. Geophys. Res.*, *115*, a12242,
309 doi:10.1029/2010ja015603.
- 310 Chen, L., R. M. Thorne, and J. Bortnik (2011), The controlling effect of ion temper-
311 ature on EMIC wave excitation and scattering, *Geophys. Res. Lett.*, *38*, l16109, doi:
312 10.1029/2011gl048653.
- 313 Cornwall, J. M. (1965), Cyclotron instabilities and electromagnetic emission in ultra low
314 frequency and very low frequency ranges, *Journal of Geophysical Research*, *70*(1), 61,
315 doi:10.1029/JZ070i001p00061.
- 316 Denton, R. E., B. J. Anderson, S. P. Gary, and S. A. Fuselier (1994), Bounded anisotropy
317 fluid model for ion temperatures, *J. Geophys. Res.*, *99*(A6).
- 318 Denton, R. E., K. Takahashi, and M. F. Thomsen (2012), O⁺ concentration at geosyn-
319 chronous orbit, Abstract SA31C-01, in *2012 Fall Meeting, AGU, San Francisco, Calif.*,
320 *3-7 Dec.*
- 321 Denton, R. E., V. K. Jordanova, and B. J. Fraser (2014), Effect of spatial density variation
322 and O⁺ concentration on the growth and evolution of electromagnetic ion cyclotron
323 waves, *J. Geophys. Res.*, *119*(10), 8372–8395, doi:10.1002/2014ja020384.
- 324 Fraser, B. J., H. J. Singer, M. L. Adrian, and D. L. Gallagher (2005), The relationship
325 between plasma density structure and EMIC waves at geosynchronous orbit, in *Inner*
326 *Magnetosphere Interactions: New Perspectives from Imaging*, *Geophys. Monog. Ser.*,
327 *vol. 159*, edited by J. L. Burch, M. Schulz, and H. Spence, pp. 55 – 70, AGU, Washing-
328 ton, D. C.

- 329 Gary, S. P., B. J. Anderson, R. E. Denton, S. A. Fuselier, and M. E. McKean (1994), A
330 limited closure relation for anisotropic plasmas from the Earths magnetosheath, *Phys.*
331 *Plasmas*, 1(5).
- 332 Halford, A. J., B. J. Fraser, and S. K. Morley (2015), EMIC waves and plasmas-
333 pheric and plume density: CRRES results, *J. Geophys. Res.*, 120, 19741992, doi:
334 10.1002/2014JA020338.
- 335 Jordanova, V. K., J. Albert, and Y. Miyoshi (2008), Relativistic electron precipitation
336 by EMIC waves from self-consistent global simulations, *J. Geophys. Res.*, 113, a00a10,
337 doi:10.1029/2008ja013239.
- 338 Kennel, C. F., and H. E. Petschek (1966), Limit on stably trapped particle fluxes, *Journal*
339 *of Geophysical Research*, 71(1), 1.
- 340 Lee, J. H., and V. Angelopoulos (2014), Observations and modeling of EMIC wave prop-
341 erties in the presence of multiple ion species as function of magnetic local time, *J.*
342 *Geophys. Res.*, 119(11), 8942–8970, doi:10.1002/2014ja020469.
- 343 Li, Z., et al. (2014), Investigation of EMIC wave scattering as the cause for the BAR-
344 REL 17 January 2013 relativistic electron precipitation event: A quantitative com-
345 parison of simulation with observations, *Geophys. Res. Lett.*, 41(24), 8722–8729, doi:
346 10.1002/2014gl062273.
- 347 Meredith, N. P., R. M. Thorne, R. B. Horne, D. Summers, B. J. Fraser, and R. R.
348 Anderson (2003), Statistical analysis of relativistic electron energies for cyclotron res-
349 onance with EMIC waves observed on CRRES, *J. Geophys. Res.*, 108(A6), 1250, doi:
350 10.1029/2002ja009700.

- 351 Ronnmark, K. (1982), Waves in homogeneous, anisotropic, multicomponent plasmas,
352 *Tech. Rep. Kiruna Geophys. Inst. Rep. 179, 56 pp.*, Swedish Institute of Space Physics,
353 Univ. of Umea, Sweden.
- 354 Shprits, Y. Y., S. R. Elkington, N. P. Meredith, and D. A. Subbotin (2008), Re-
355 view of modeling of losses and sources of relativistic electrons in the outer radia-
356 tion belt i: Radial transport, *J. Atmos. Sol.-Terr. Phys.*, *70*(14), 1679–1693, doi:
357 10.1016/j.jastp.2008.06.008.
- 358 Silin, I., I. R. Mann, R. D. Sydora, D. Summers, and R. L. Mace (2011), Warm plasma
359 effects on electromagnetic ion cyclotron wave MeV electron interactions in the magne-
360 tosphere, *J. Geophys. Res.*, *116*, a05215, doi:10.1029/2010ja016398.
- 361 Swanson, D. G. (2003), *Plasma Waves*, 2nd ed., Institute of Physics Publishing, Bristol
362 and Philadelphia.
- 363 Ukhorskiy, A. Y., Y. Y. Shprits, B. J. Anderson, K. Takahashi, and R. M. Thorne (2010),
364 Rapid scattering of radiation belt electrons by storm-time emic waves, *Geophys. Res.*
365 *Lett.*, *37*, 109101, doi:10.1029/2010gl042906.
- 366 Usanova, M. E., F. Darrouzet, I. R. Mann, and J. Bortnik (2013), Statistical analysis
367 of EMIC waves in plasmaspheric plumes from Cluster observations, *J. Geophys. Res.*,
368 *118*(8), 4946–4951, doi:10.1002/jgra.50464.

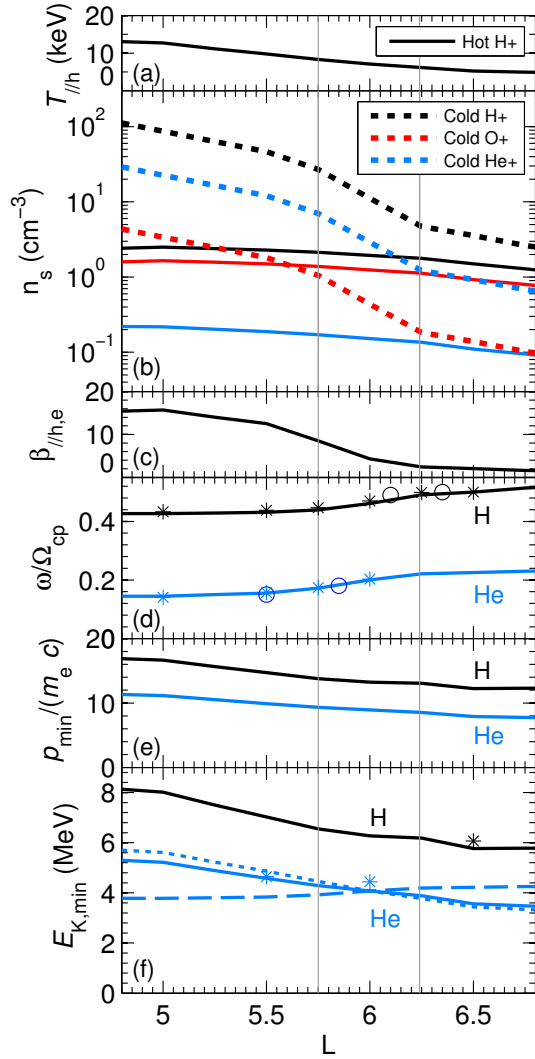


Figure 1. Using parameters from the ring current simulation described by *Denton et al.* [2014], (a) $T_{\parallel h}$ for hot H+, (b) density n_s for different particle species s (solid curves for hot populations and dotted curves for cold populations) in cm^{-3} , (c) hybrid plasma beta $\beta_{\parallel h,e}$, (d) $\bar{\omega} \equiv \omega/\Omega_{\text{cp}}$ for H band EMIC (black solid curve) and He band EMIC (blue solid curve), and (e) $\bar{p}_{\text{min}} \equiv p_{\text{min}}/(m_e c)$ and (f) minimum resonant kinetic energy $E_{K,\text{min}}$ (solid curves) for interaction of relativistic electrons with the wave frequencies that were plotted in panel c; these are all plotted versus L . The other symbols in the plot are described in the text.

D R A F T

July 14, 2015, 12:13pm

D R A F T

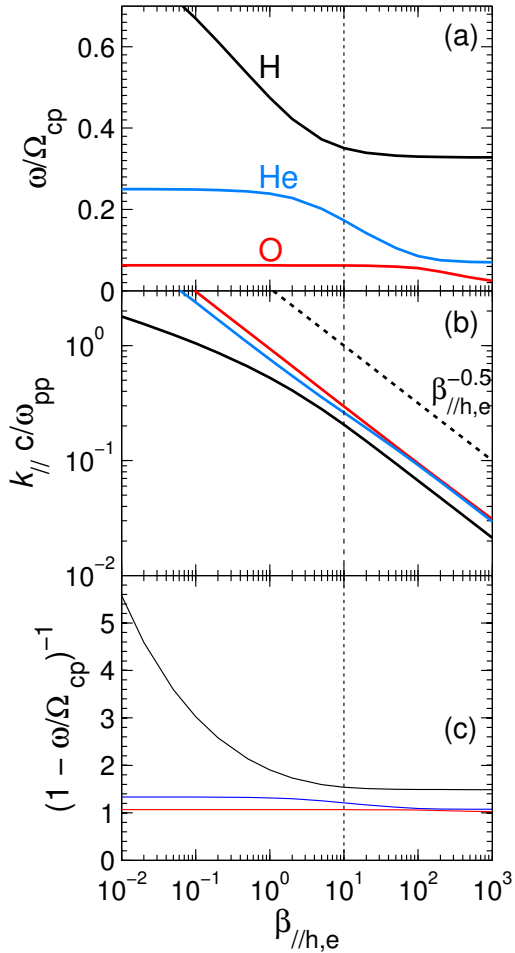


Figure 2. Holding $\eta_{\text{He}^+} = 0.1$ and $\eta_{\text{O}^+} = 0.01$ constant, (a) $\bar{\omega}$, (b) \bar{k}_{\parallel} , and (c) $(1 - \bar{\omega})^{-1} = (\bar{k}_{\parallel} \sqrt{\beta_{\parallel h,e}})^{-1}$ versus $\beta_{\parallel h,e}$. Black, blue, and red color correspond respectively to the H, He, and O band EMIC modes. In (b), the diagonal dotted black curve is proportional to $\beta_{\parallel h,e}^{-0.5}$. The vertical dotted black line is at the nominal value of $\beta_{\parallel h,e} = 10$ relevant for other plots.

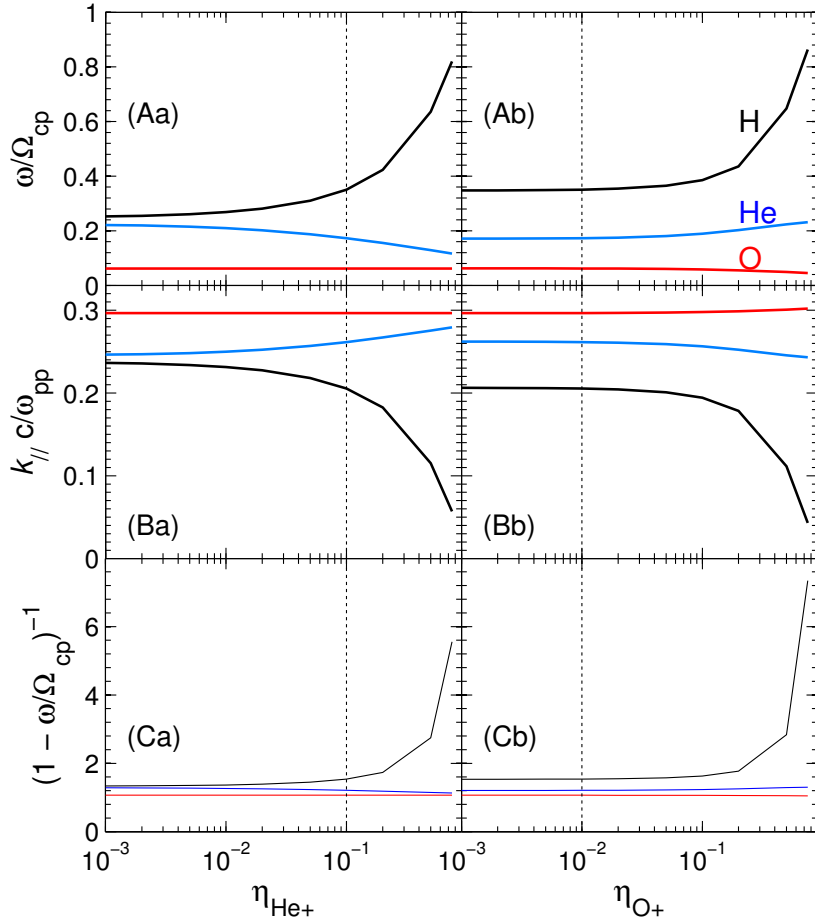


Figure 3. Same quantities as were plotted in Figure 2, but plotted versus η_{He^+} holding $\eta_{\text{O}^+} = 0.01$ constant in column a, and versus η_{O^+} holding $\eta_{\text{He}^+} = 0.1$ constant in column b. In both cases, $\beta_{\parallel \text{h,e}} = 10$ is constant. The vertical dotted black lines are plotted at the nominal values used in other plots, $\eta_{\text{He}^+} = 0.1$ in column a, and at $\eta_{\text{O}^+} = 0.01$ in column b.